Mass synthesis of high performance $(La_{0.75}Sr_{0.25})_{0.95}MnO_{3\pm\delta}$ nano-powder prepared via a low-carbon chemical solution method

CrossMark

Jian Xin Wang [a,*], Jia Long Sun [a], Chang Rong He [a], Qin Wang [b], Wei Guo Wang [a,1]

[a] Division of Fuel cell and Energy Technology, Ningbo Institute of Materials, Technology & Engineering, Chinese Academy of Sciences, Ningbo 315201, PR China
[b] Department of Microelectronic Science and Engineering, Faculty of Science, Ningbo University, Ningbo 315211, PR China

HIGHLIGHTS

- A low-carbon chemical solution method is established and scaled up to prepare high performance LSM powders.
- The organic compound emission is reduced to a quarter of that in the citric acid–nitrate method.
- The conductivity of the sintered LSM is about 220 S cm^{-1} in air at 700–1000 °C.
- As-prepared symmetric and unit cells with LSM–YSZ cathode show excellent performance.

ARTICLE INFO

ABSTRACT

A novel low-carbon chemical solution method is established and successfully scaled up to prepare $(La_{0.75}Sr_{0.25})_{0.95}MnO_{3\pm\delta}$(LSM) nano-powders, in which acetate and acrylic acid have been used as raw materials. Distinguish from the traditional chemical solution methods, nitrate and amino compound are non-used in this method and without causing any fire hazard or explosion condition which are usually found in most of the solution synthesis reactions. The organic compound emission is reduced to a quarter of that in the citric acid–nitrate method. This optimization is attributed to the low application amount and high effect of acrylic acid by means of the co-operation of ethylenic linkage and carboxyl group. As-prepared powders are high purity, single phase, slight aggregation with grain size less than 100 nm. The conductivity of the sintered LSM sample is measured about 220 S cm^{-1} in air at 700–1000 °C. The polarization resistance of LSM–YSZ cathode is less than 0.1 Ω cm^2 at 800 °C. Anode supported Cells with configuration of Ni + YSZ/YSZ/LSM + YSZ exhibit the power density of 0.54 W cm^{-2} at 800 °C and 0.7 V. These results indicate that the novel acetate–acrylic method is very suitable for mass synthesis of high performance LSM powders.

1. Introduction

Perovskite-type strontium doped lanthanum manganite ($La_{1-x}Sr_xMnO_{3-\delta}$ abbreviated as LSM) is of interest for several possible applications due to its unique physical chemical properties such as catalysis [1–5], giant magneto-resistance (GMR) [6,7], and possibly for use as cathode materials for solid-oxide fuel cell (SOFC) [8–16].

It is well known that the properties of perovskite particles are strongly influenced by their compositions and microstructures, which are sensitive to the preparation methodologies. Various methods have been used to prepare LSM powders, solid state reaction is a conventional method [5,17,18], the powders made by this method usually have larger particle size and poorer catalytic activity. The solution chemistry methods are the state-of-the-art methods, such as combustion synthesis [8–10], co-precipitation [6,7,11,12], cellulose–glycine nitrate process (GNP) [13], spray pyrolysis [14], sol–gel and Pechini [15], they provide interesting alternatives because the mixing of species occurs on the atomic scale, cations being dissolved in solution may give rise to more homogeneous nano-powder with controlled stoichiometry.

However, for the different chemical behavior of each cation, these synthetic procedures cannot be applied to large-scale (above 1 kg) and economic production because they require expensive and often toxic reagents [19], complicated synthetic steps, and high reaction temperature and long time. For example:

* Corresponding author. Tel.: +86 574 8791 0735; fax: +86 574 8669 5470.
E-mail addresses: jxwang@nimte.ac.cn (J.X. Wang), wgwang@nimte.ac.cn (W.G. Wang).
[1] Tel.: +86 574 8791 1363; fax: +86 574 8668 5846.

in our lab, a modified Pechini method [15] was established and used to prepare high performance LSM nano-powder about 500 g per batch, five years ago. But, when the synthetic amount was increased to above 1 kg per batch, this method was no longer in force for the reason of predecessor explosion or flame.

To the best of our knowledge, there is no report on preparation of LSM nano-powder by in situ polymerization of the mixed aqueous solution of acrylic acid in the absent of nitrate followed by a pyrolysis process. This method has the advantage that it can be readily scaled up in the form of a batch process producing highly homogeneous LSM nano-powder with excellent electrical performance.

In this paper, a novel acetate–acrylic polymer-pyrolysis method was established and successfully scaled up to prepare about 6 kg LSM nano-powder with a yield above 95%. Distinguish from the traditional chemical solution method, nitrate and amino compound were non-used in this method and without causing any fire hazard or explosion condition which are usually found in most of the solution synthesis reactions. The microstructure and electrical characteristics of the LSM powders were studied and discussed.

2. Experimental

2.1. Powder synthesis and characterization

Nanocrystalline LSM powders were prepared by a novel acetate–acrylic polymer-pyrolysis method, in which lanthanum oxide, strontium acetate, manganese acetate, acetic acid and acrylic acid were used as raw materials. Briefly, the solutions with stoichiometric ratio $(La_{0.75}Sr_{0.25})_{0.95}MnO_{3\pm\delta}$ of lanthanum acetate, strontium acetate, manganese acetate were prepared separately and mixed with gentle stirring. Different amount of acrylic acid with the mole ratio to overall metal ions (L/M) of 0.3, 0.6, 1.2 and 2.4 were added to the solution respectively to study the influence on morphology and structure of the oxide particles. The mixtures were kept in a water bath at 80 °C with constant stirring until gelation was completed, and then the as-prepared gels were dried at 120 °C and 250 °C, respectively. The ultrafine LSM powders were obtained by calcining the dried gel at 500, 600, 800 and 950 °C for 5 h.

To study the pyrolysis behavior and the phase evolution of the gel precursor dried at 120 °C, TG/DTA analysis was carried out with heating velocity of 5 °C min^{-1} in air. Phase formation and crystallinity of the resulting powders were characterized by means of X-ray diffraction (XRD) in a Bruker D8 Advance with Cu Kα radiation. The microstructures of the LSM powders and sintered samples were observed by field emission scanning electron microscope (SEM, Hitachi S4800) and the high resolution transmission electronic microscopy (HR-TEM, Tecnai F20, FEI, USA). The purity of the synthesized LSM powders was measured by XRF (Rigaku ZSX Primus II). Specific surface areas of LSM powders were measured by the Brunauer–Emmett–Teller (BET) isotherm technique with nitrogen adsorption using a Micromeritics ASAP 2020M physisorption analyzer. Particle size distribution (PSD) analysis was made by Zatasizer nano ZS Malvern Instruments Ltd. (UK).

The nanocrystalline LSM powders sintered at 950 °C for 5 h were grounded by hand for about 1 h. Pressed bars of 25 mm × 8 mm × 3 mm were shaped by uniaxial pressing at a pressure of about 200 MPa, and then sintered at 1250 °C for 5 h. The electrical conductivity of the sintered LSM samples was measured by four probe DC measurement in the temperature range of 25–1000 °C in air.

2.2. Symmetric and unit cells fabrication and measurement

The symmetric cells with configuration of LSM + YSZ/YSZ/LSM + YSZ, anode supported cells with configuration of Ni + YSZ/YSZ/LSM + YSZ were prepared and measured. The half cell was produced by tape casting the anode support, spraying the NiO + YSZ active anode and YSZ electrolyte layer, followed by co-sintering. The thicknesses of the sintered anode support, active anode and electrolyte layers are about 450, 15 and 10 μm, respectively. The NiO and YSZ were commercial powders, TZ-8Y (ZrO$_2$ with 8 mol% Y$_2$O$_3$, Tosoh Corporation). The LSM powders with the nominal compositions $(La_{0.75}Sr_{0.25})_{0.95}MnO_{3\pm\delta}$ have been produced by the acetate–acrylic polymer-pyrolysis method. The ethanol based slurry of LSM and YSZ was produced by ball milling and sprayed on both sides of a sintered YSZ foil with the thickness of approximately 200 μm and one side of the Ni + YSZ/YSZ/half cells, then sintered at 1100 °C for 2 h. The sintered symmetric cells were painted with platinum paste and cut to dimensions of 7.1 mm × 7.1 mm. The tests were performed as two-electrode four-wire measurements, and the polarization resistance was determined as half of the measured electrode polarization resistance [15]. Impedance measurements were carried out using a Solartron 1260 frequency response analyzer over the frequency range from 2 MHz to 0.1 Hz and 20 mV excitation voltage at 650–850 °C in air. The microstructure of the sintered cells was investigated using the FESEM (Hitachi SU70). As-prepared unit cell with an active electrode area of 4 × 4 cm^2 was tested in a stainless steel test–house using dry hydrogen as fuel and air as oxidant.

3. Results and discussion

3.1. Results of LSM powders research

The XRD patterns of the LSM powders prepared using different L/M values are shown in Fig. 1. All powder samples were calcined at 950 °C for 5 h. For three kinds of powders with L/M = 0.6, 1.2, 2.4, only the XRD patterns of crystalline $La_{0.74}Sr_{0.26}MnO_3$ (PDF Number: 00-056-0616) were observed, while for the powders with L/M = 0.3, besides $La_{0.74}Sr_{0.26}MnO_3$ phase, the presence of La_2O_3 phase was observed in the XRD patterns. The average crystallite size of the powders prepared in this study was about 30 nm as deduced from the XRD pattern by Debye–Scherer equation after subtraction of the equipment widening.
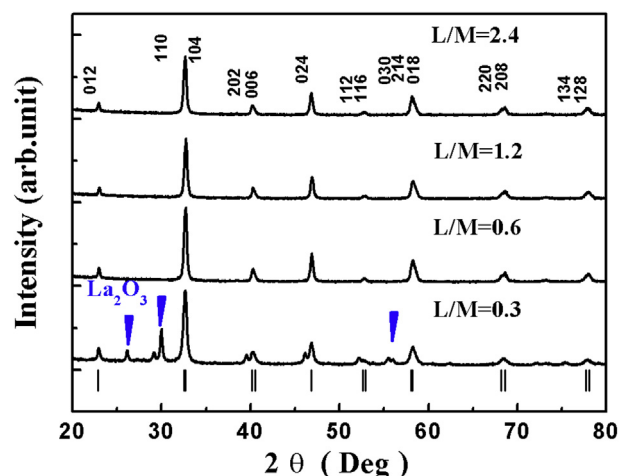

Fig. 1. The XRD patterns of the LSM powders prepared using different L/M values.

It suggests that a precursor solution with L/M ≥ 0.6 seems to favor the chelation between metal ions and acrylic acid and facilitate the crystallization. The L/M value of the solution has an evident effect on the chelating process. For the citric acid−nitrate method (CA) the mole ratio of citric acid to overall metal ions (L/M) usually above 2. However in this experiment the application amount of acrylic acid can be as low as L/M = 0.6. It can be explained as follow: The acrylic acid is an organic acid with conjugated double bond. The carbon−carbon double bond in AA conjugated with the double bond of carbon−oxygen double bond. This conjugated double bond leads to a delocalization effect on the whole molecule. This makes the electron density of the oxygen atom in the acrylic acid reduce. As a consequence of this delocalization effect, the complexing of the acrylic acid with the metal ions weakened when compared to the poly acrylic acid (PAA). The mix solution of AA and metal acetates was heated in an 80 °C water bath and the AA polymerized into PAA by thermal initiation through a free radical polymerization. Then the PAA complexing with the metal ions. The mix solution turned into a gel. So, the low application amount and high effect of acrylic acid are attributed to the co-operation of ethylenic linkage and carboxyl group [20].

The SEM images of the LSM powders prepared using different L/M values are shown in Fig. 2. All powder samples were calcined at 950 °C for 5 h. It's obvious that the morphology of these four LSM powders is not significantly dependent on the L/M value. All LSM powders have few aggregates, the particles are spherical and the particle size is about 100 nm with a narrow distribution. The particle usually included several crystalline grains, so the particle size measured from SEM, TEM and PSD is always larger than the average crystalline grain size calculated from the XRD. From SEM images showed in Fig. 2, it can be seen that fine morphology of LSM powders can be obtained in a wide range of the dosage acrylic acid. For the samples with low application amount such as: L/M = 0.3, 0.6, the high effect of acrylic acid are attributed to the co-operation of ethylenic linkage and carboxyl group [20,21].

As a whole, in this experiment the optimization conditions of prepared the LSM powders are using acrylic acid as complexing

agent, and L/M = 0.6. Furthermore, this preparation process was successfully scale up to prepare 6.6 kg LSM nano-powder.

In order to seek the essential distinguish, the flow charts of LSM powder synthesis by Pechini: citric acid−nitrate method (CA) [15] and acetate−acrylic polymer-pyrolysis (AA) method are showed in Fig. 3. There are two main differences, first is the metal−salt, for CA method lanthanum nitrate, strontium nitrate and manganese nitrate are used, while for AA method lanthanum acetate, strontium acetate and manganese acetate are used as source materials. The second difference is for CA method citric acid and ethylene glycol are used, while for AA method only acrylic acid is used as additive agent.

TG/DTA curves of LSM-CA and LSM-AA precursors dried at 120 °C are showed in Fig. 4. For the TG curve of LSM-CA, there are three main weight loss steps, the first weight loss about 20% occurs during the heating step from room temperature to 150 °C, resulting from the dehydration. The second weight loss step is from 150 °C to 250 °C with a weight loss of about 40% is observed, which corresponds to the decomposition of nitrates. The third weight loss step is from 250 °C to 400 °C with another 20% weight loss, which corresponds to the decarbonization of the residual organic compound. The DTA curve of LSM-CA reveals two strong and sharp exothermic peaks with vertex at 240 °C and 350 °C, which are likely due to the decomposition of nitrates and combustion of the chelate complex, respectively. For the TG curve of LSM-AA, there are only two main weight loss steps, the first weight loss about 10% occurs during the heating step from room temperature to 150 °C, resulting from the dehydration. The second weight loss step is from 250 °C to 400 °C with a weight loss of about 40% is observed, which corresponds to the decomposition of acetates and the decarbonization of the residual organic compound. The DTA curve of LSM-AA reveals one strong and sharp exothermic peak with a vertex at 360 °C, which is likely due to the decomposition of acetates and combustion of the chelate complex. Above 400 °C the TG-DTA curves shows no further endo- or exo-thermal peak, and very little weight loss was observed. The absence of nitrates in LSM-AA method can avoid nitrate violent thermolysis and restrain the volumetric expansion
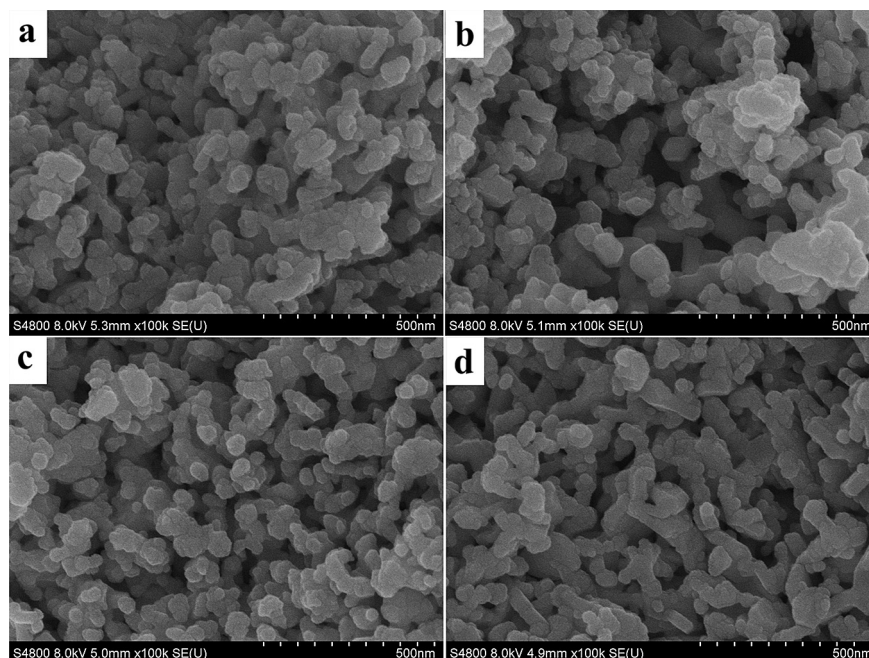

Fig. 2. The SEM images of the LSM powders prepared using different L/M values, (a) L/M = 0.3, (b) L/M = 0.6, (c) L/M = 1.2, (d) L/M = 2.4.
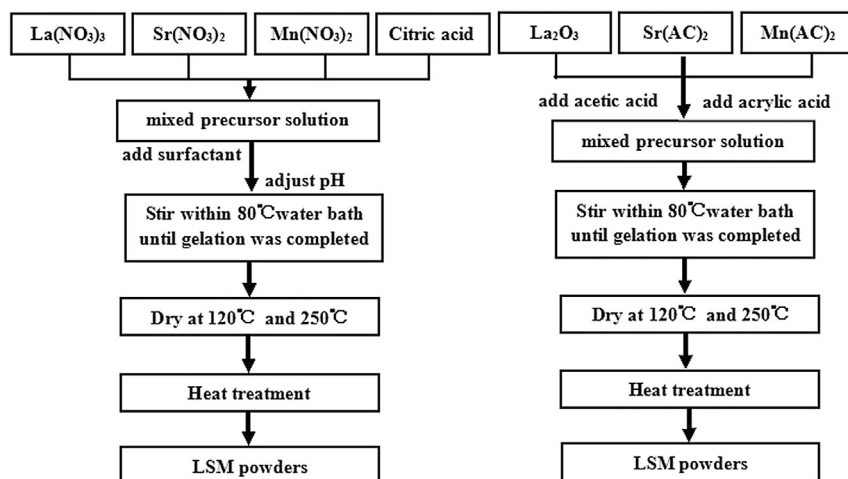
Fig. 3. Flow charts of LSM powder synthesis by CA (left) and AA (right) method.

and fierce combustion phenomena. The total weight loss of LSM-AA is about 50%, that means the ratio of weight loss to outcome is 1:1, while the total weight loss of LSM-CA is about 80%, that means the ratio of weight loss to outcome is 4:1, so to obtain the same outcome, the organic compound emission of AA method is only a quarter of that in CA method. This optimization is attributed to the replace citric acid with acrylic acid, which can heavily reduce carboxylic acid application amount. The low application amount and high effect of acrylic acid are attributed to the co-operation of ethylenic linkage and carboxyl group [20,21].

The XRD patterns of the LSM-AA powders calcined at 500, 600, 800 and 950 °C are shown in Fig. 5. It can be seen that the powders calcined at 500 °C consists of amorphous materials, while powders calcined above 600 °C have well crystallized perovskite structure of LSM and obvious La$_2$O$_3$ impurity phase. Although a small amount of La$_2$O$_3$ phase could be observed in the pattern of powders calcined at 800 °C, the impurity phase totally disappears and a single perovskite phase is formed completely when the sintering temperature reaches 950 °C. It can be seen that with an increase in the calcination temperature, the intensity of peaks increases and the diffraction peaks become sharper and narrower, which indicate that the crystallite size of the LSM powders grown larger gradually.

The TEM images shown in Fig. 6 correspond to four kinds of the LSM-AA powders calcined at 500, 600, 800 and 950 °C. It can be see that all powders have few aggregates, and the particles are spherical and the particle sizes are less than 100 nm with a narrow distribution. With the increase of the calcination temperature, LSM powders grow larger gradually, from less than 20 nm at 500 °C to about 80 nm at 950 °C.

Then the LSM powders as-prepared were characterized by XRF, BET and PSD analysis. The XRF results show that the LSM powders are composed of La$_2$O$_3$ 55.3 wt%, MnO 32.1 wt%, SrO 12.6 wt%, which indicate that the powders composition is near the nominal (La$_{0.75}$Sr$_{0.25}$)$_{0.95}$MnO$_{3\pm\delta}$, the purity of the LSM powders is higher than 99.9%. The special surface area of the LSM powders is found to be 5.7 m^2 g^{-1} at the calcination temperature of 950 °C and 10.6 m^2 g^{-1} after ball-milled 4 h. Using the surface area and assuming all particles are spherical, the average particle size (D_{BET}) can be estimated as 86 nm, using the equation [22]:

$$D_{BET} = \frac{6}{\rho S_v}$$

Where ρ is the density of LSM (6.6 g cm^{-3}) and S_v is the surface area of the sample. The result is in good agreement with the observed particle size from FESEM, TEM and XRD, suggesting the majority of particles are nano-structured. PSD analysis shows that the particle size of LSM powders are around 200–300 nm with a narrow distribution.
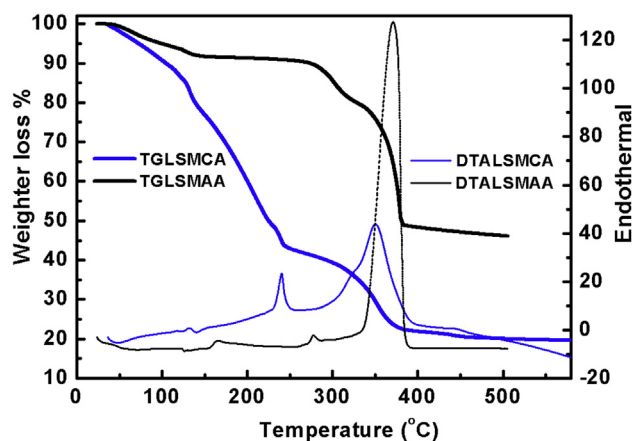

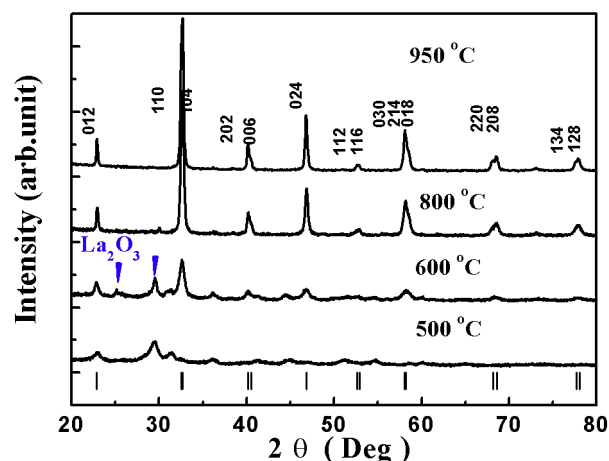**Fig. 4.** TG/DTA curves of the as-synthesized LSM precursors dried at 120 °C.

Fig. 5. The XRD patterns of the LSM-AA powders calcined at 500, 600, 800 and 950 °C.
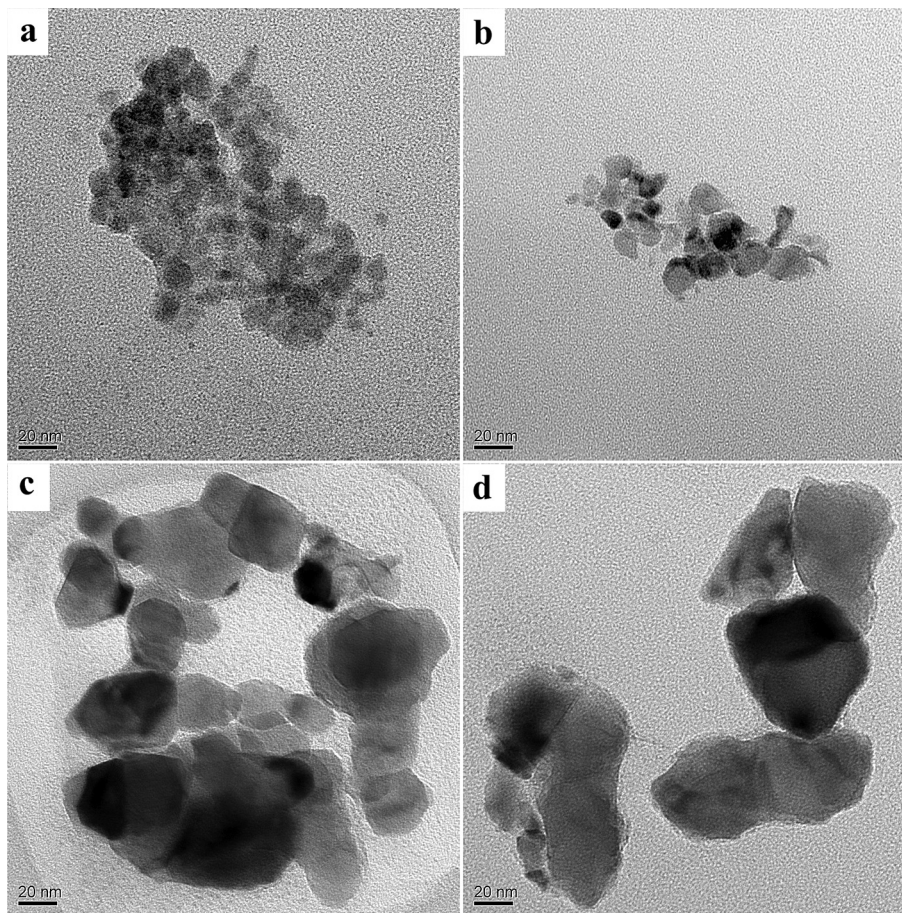
Fig. 6. TEM photos of the LSM-AA powders calcined at (a) 500, (b) 600, (c) 800 and (d) 950 °C.

In view of all characterizations of the LSM-AA powders, it can be concluded that the process optimization has lead a high purity, single phase, homogenous and slight aggregation LSM-AA powders with grain size less than 100 nm.

3.2. Electrical conductivity of the LSM bulk

Fig. 7 shows the electrical conductivity of the sintered LSM samples LSM-AA from the acetate-acrylic method and LSM-CA from pechini method [15], respectively. Obvious phase transition is observed in the thermal dependence of the conductivity at about 80 °C on both sintered $(La_{0.75}Sr_{0.25})_{0.95}MnO_{3\pm\delta}$ samples. Both curves show the same tendency and can be divided into three stages. In the first stage, from 30 °C to 80 °C, the conductivities show a metallicity, which rapidly drop accompany the increase of temperature. In the second stage, from 80 °C to 700 °C, the conductivities continuous ascend accompany the increase of temperature and show a typical semiconductor feature. Similar results, the conductivities of sintered $(La_{0.75}Sr_{0.25})MnO_3$ sample continuous ascend from about 110 S cm^{-1} at 500 K to about 180 S cm^{-1} at 1000 K, reported by Takanori Itohc et al. [23]. The conductivity mechanism of the second stage can be attributed to the hopping of p-type small polarons. In the third stage, from 700 °C to 1000 °C, the conductivities reach a platform and ascend very slow accompany the increase of temperature. In this temperature range, both samples exhibit high electronic conductivity, LSM-AA is almost 220 S cm^{-1}, while the conductivity of LSM-CA is around 200 S cm^{-1} [15]. The high conductivity of the LSM-AA sample could be attributed to the excellent performance of nanocrystalline powders prepared from the acetate-acrylic method.

3.3. Cell performance

Fig. 8 displays the fracture cross-section morphology of LSM–YSZ cathode sintered at 1100 °C-2 h. The coat is about 20 μm thick and has a homogeneous porous structure composited with LSM, YSZ and pores. The LSM and YSZ grains are clear and round with
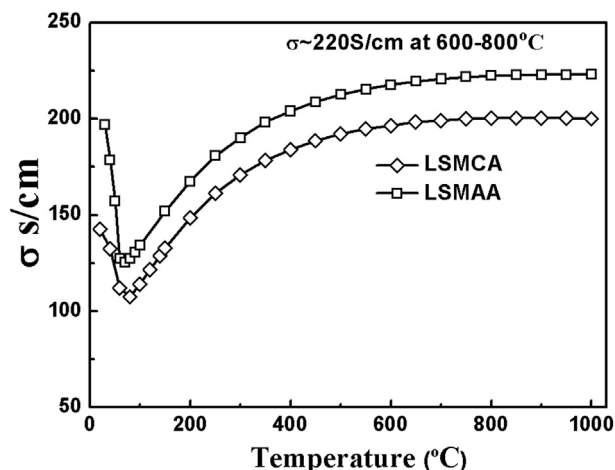

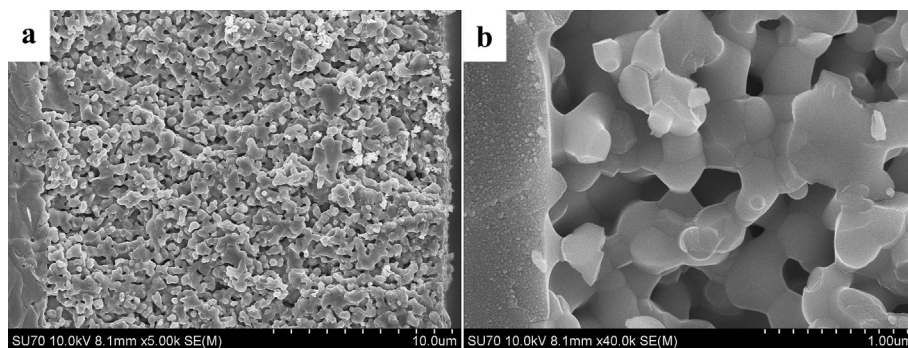**Fig. 7.** The electrical conductivity of the sintered LSM samples.

Fig. 8. The cross-section SEM pictures of the LSM−YSZ cathode sintered at 1100 °C-2 h.

grain size less than 400 nm, they were sintered together forming a 3D network, the LSM and YSZ phases cannot be distinguished clearly for the reason of their backscattered coefficients are very close to each other. The sintering necks between the grains are thickset, which indicates good connection between LSM/LSM, LSM/YSZ and YSZ/YSZ grains. Furthermore, the LSM−YSZ coat is firmly adhered to the YSZ substrate. It can be seen that all the available "branches" of the coat at the interfacial region are firmly connected to the YSZ substrate. Such sturdy and homogeneous porous structure can offer strong and large extended contacts between ionic conductor electrolyte YSZ, electronic conductor LSM and the pore, which will enlarge the number of the active TPBs of the cathode.

In our previous work [15], similar nanostructure structure of LSM−YSZ composite cathode was obtained from LSM-CA powder and sintered at 1000 °C-2 h. The main differences are the grain size is finer (about 200 nm), while the connection is not enough strong, when compared to the structure of LSM−YSZ cathode from LSM-AA powder sintered at 1100 °C-2 h in this work. The connection of electrode and electrolyte is much important for a unite cell, which means stably operated performance.

The area specific polarization resistance of less than 0.2 Ω cm^2 at 750 °C and 0.1 Ω cm^2 at 800 °C have been achieved in symmetric cells with the LSM−YSZ sintered at 1100 °C. This polarization resistance is slightly larger than that (0.175 Ω cm^2 at 750 °C) of LSM−YSZ cathode obtained from LSM-CA powders [15]. This is attributed to the lower porosity and larger aggregation of particle in the LSM−YSZ cathode from LSM-AA powders sintered at 1100 °C than that from LSM-CA powders sintered at 1000 °C. This performance indicates that the anode supported cell with the LSM−YSZ composite cathode prepared from LSM-AA powder and sintered at 1100 °C has the potential to be stably operated with a satisfactory power density.

An YSZ-based anode-supported SOFC was fabricated in the configuration of NiO−YSZ/YSZ/LSM−YSZ. The cathode was sintered at 1100 °C and the active electrode area was 4 × 4 cm^2. Fig. 9 shows the I−V curves and corresponding power densities of the cell. Unit cell was tested in a stainless steel test−house using dry hydrogen as fuel and air as oxidant (H$_2$:Air = 800:2000 Sc cm). The open cell voltage reaches 1.1 V, which indicates the tight electrolyte, good cell sealing and optimal electrical potential through the cell. The I−V curves exhibits the power density of 0.54 W cm^{-2} at 800 °C and 0.8 W cm^{-2} at 850 °C (H$_2$/air, 0.7 V, active electrode area of 4 × 4 cm^2), respectively. These performances are almost as same as that of the anode-supported cells reported in our previous work [24], in which LSM−YSZ cathode was obtained from LSM-CA powders. These results indicate that the LSM-AA powders are very suitable for synthesis of high performance LSM−YSZ cathode.

4. Conclusion

In this study, a novel acetate−acrylic polymer-pyrolysis method was established and successfully scaled up to prepare about 6 kg (La$_{0.75}$Sr$_{0.25}$)$_{0.95}$MnO$_{3\pm\delta}$ (LSM) nano-powder with a high yield above 95%, in which lanthanum oxide, strontium acetate, manganese acetate, acetic acid and acrylic acid have been used as raw materials. Distinguish from the traditional chemical solution method, nitrate and amino compound were non-used in this method and without causing any fire hazard or explosion condition which are usually found in most of the solution synthesis reactions. To obtain the same outcome, the organic compound emissions of AA method is only a quarter of that in CA method. This optimization is attributed to the replace citric acid with acrylic acid, which can heavily reduce carboxylic acid application amount. The low application amount and high effect of acrylic acid are attributed to the co-operation of ethylenic linkage and carboxyl group. Microstructure characterizations show that as-prepared powders are high purity, single phase, slight aggregation with grain size less than 100 nm. The conductivity of the sintered LSM sample prepared from this powders was measured about 220 S cm^{-1} in air at 600−800 °C. The area specific polarization resistance of less than 0.2 Ω cm^2 at 750 °C and 0.1 Ω cm^2 at 800 °C have been achieved in symmetric cells with the LSM−YSZ cathode sintered at 1100 °C. Anode supported Cells with configuration of Ni + YSZ/YSZ/ LSM + YSZ exhibited the power density of 0.54 W cm^{-2} at 800 °C and 0.8 W cm^{-2} at 850 °C (H$_2$/air, 0.7 V, active electrode area of 4 × 4 cm^2), respectively. These results indicate that the novel acetate−acrylic method is very suitable for mass synthesis of high performance LSM powders. Given the advantage and easiness of
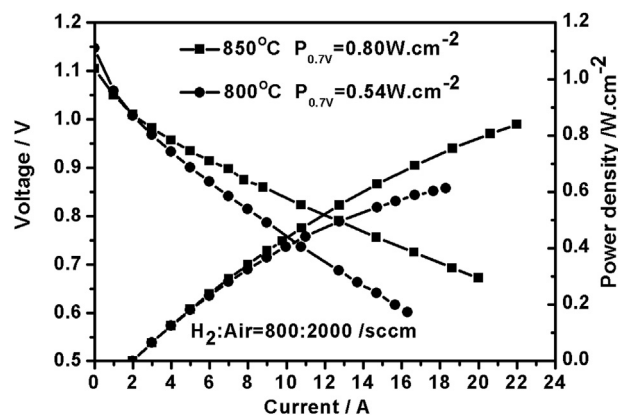

Fig. 9. I−V characteristics of anode-supported Ni + YSZ/YSZ/LSM + YSZ cell.

this method it can be considered that this approach could be applied to many other oxide systems.

Acknowledgments

References

[1] Samaneh Taherian, Mohammad H. Entezari, Narjes Ghows, Ultrason. Sonochem. 20 (2013) 1419—1427.
[2] V. Roche, A. Hadjar, J.P. Deloume, T. Pagnier, R. Revel, C. Roux, E. Siebert, P. Vernoux, Catal. Today 146 (2009) 266—273.
[3] Carlo Resini, Federico Catania, Silvia Berardinelli, Ombretta Paladino, Guido Busca, Appl. Catal. B Environ. 84 (2008) 678—683.
[4] B. Morel, R. Roberge, S. Savoie, T.W. Napporn, M. Meunier, Appl. Catal. A Gen. 323 (2007) 181—187.
[5] Takashi Hibino, Kazuo Suzuki, Ken-ichi Ushiki, Yoshitaka Kuwahara, Mitsukuni Mizuno, Appl. Catal. A Gen. 145 (1996) 297—306.
[6] X.L. Jiang, Y.J. Yao, M. Lai, D.S. Jacob, A. Gedanken, Y.W. Du, Supercond. Nov. Magn. 26 (2013) 1385—1390.
[7] Guangsheng Pang, Xiaonong Xu, Vladimir Markovich, Sigalit Avivi, et al., Mater. Res. Bull. 38 (2003) 11—16.
[8] K. Prabhakaran, Jorly Joseph, N.M. Gokhale, S.C. Sharma, Ramji Lal, Ceram. Int. 31 (2005) 327—331.
[9] Leandro da Conceic, Nielson F.P. Ribeiro, Jose Geraldo M. Furtado, Mariana M.V.M. Souza, Ceram. Int. 35 (2009) 1683—1687.
[10] Chenghao Yang, Adam Coffin, Fanglin Chen, Int. J. Hydrogen Energy 35 (2010) 3221—3226.
[11] M. Balaguer, V.B. Vert 1, L. Navarrete, J.M. Serra, J. Power Sources 223 (2013) 214—220.
[12] Chao Jin, Xuecheng Cao, Liya Zhang, Cong Zhang, Ruizhi Yang, J. Power Sources 241 (2013) 225—230.
[13] Jungdeok Parka, Jing Zoua, Jongshik Chung, J. Power Sources 195 (2010) 4593—4599.
[14] Akifusa Hagiwara, Natsuro Hobara, Koichi Takizawa, Kazuyoshi Sato, Hiroya Abe, Makio Naito, Solid State Ionics 178 (2007) 1123—1134.
[15] Jian XinWang, You Kun Tao, Jing Shao, Wei Guo Wang, J. Power Sources 186 (2009) 344—348.
[16] W.G. Wang, Y.-L. Liu, R. Barfod, S.B. Schougaard, P. Gordes, S. Ramousse, P.V. Hendriksen, M. Mogensen, Electrochem. Solid-State Lett. 8 (12) (2005) A619—A621.
[17] K.R. Nagde, S.S. Bhoga, Ionics 16 (2010) 361—370.
[18] Tongan Jin, Kathy Lu, J. Power Sources 196 (2011) 8331—8339.
[19] A. Tarancon, G. Dezanneau, J. Arbiol, F. Peiro, J.R. Morante, J. Power Sources 118 (2003) 256—264.
[20] Ai Zhu Liu, Jian Xin Wang, Chang Rong He, He Miao, Yi Zhang, Wei Guo Wang, Ceram. Int. 39 (2013) 6229—6235.
[21] Xian-Ming Liu, Guo Yang, Shao-Yun Fu, et al., Mater. Sci. Eng. 27 (2007) 750—755.
[22] Jing Shao, Youkun Tao, Jianxin Wang, Cheng Xu, Wei GuoWang, J. Alloys Compd. 484 (2009) 263—267.
[23] Takanori Itoh, Saori Shirasaki, Yoshinori Fujie, Naoto Kitamura, Yasushi Idemoto, Keiichi Osaka, Hironori Ofuchi, Sayaka Hirayama, Tetsuo Honma, Ichiro Hirosawa, J. Alloys Compd. 491 (2010) 527—535.
[24] Jian Xin Wang, Jing Shao, You Kun Tao, Wei Guo Wang, ECS Trans. 25 (2) (2009) 595.